Inhibition of Cathepsin K with Lysosomotropic Macromolecular Inhibitors†

Dong Wang,‡ Michal Pechar,‡,§,|| Weijie Li,§,⊥ Pavla Kopečková,‡ Dieter Brömme,⊥ and Jindřich Kopeček*,‡,#

Department of Pharmaceutics and Pharmaceutical Chemistry/CCCD and Department of Bioengineering, University of Utah, Salt Lake City, Utah 84112, and Department of Human Genetics, Mount Sinai School of Medicine, New York, New York 10029

Received February 20, 2002; Revised Manuscript Received May 6, 2002

ABSTRACT: Cathepsin K is the major enzyme responsible for the degradation of the protein matrix of bone and probably for the destruction of articular cartilage in rheumatoid arthritis joints. These processes occur mainly in the resorption lacuna and within the lysosomal compartment. Here, we have designed, synthesized, and evaluated new lysosomotropic (water-soluble) polymer−cathepsin K inhibitor conjugates. In particular, we characterized the relationship between conjugate structures and their activity to inhibit cathepsins K, B, L, and papain. A potent selective cathepsin K inhibitor, 1,5-bis(*N*-benzyloxycarbonyl-leucyl)carbohydrazide, was modified to 1-(*N*-benzyloxycarbonylleucyl)-5-(phenylalanylleucyl)carbohydrazide (**I**) to facilitate polymer conjugation. It was conjugated to the polymer chain termini of two water-soluble polymers {α-methoxy poly(ethylene glycol), abbreviated as mPEG−**I**; semitelechelic poly[*N*-(2-hydroxypropyl)methacrylamide], abbreviated as ST-PHPMA−**I**}. The conjugation of inhibitor **I** to *N*-(2-hydroxypropyl)methacrylamide (HPMA) copolymer side chains was accomplished via either a Gly−Gly spacer (PHPMA−GG−**I**) or with no spacer between **I** and the copolymer backbone (PHPMA−**I**). Kinetic analysis revealed that free inhibitor **I** possessed an apparent second-order rate constant against cathepsin K (k_{obs}/[I] = 1.3×10^6 M^{-1} s^{-1}) similar to that of unmodified 1,5-bis(Cbz−Leu) carbohydrazide, while **I** conjugated to the chain termini of mPEG and ST-PHPMA−COOH had slightly lower values (about 5×10^5 M^{-1} s^{-1}). The k_{obs}/[I] values for **I** attached to the side chains of HPMA copolymers (PHPMA−GG−**I** and PHPMA−**I**) were about 3×10^4 M^{-1} s^{-1}. When tested against cathepsin L, inhibitor **I** and all its polymer conjugates produced k_{obs}/[I] values 1−2 orders of magnitude less than those determined for cathepsin K, while for cathepsin B and papain, the values were 2−4 orders of magnitude lower. The ability of mPEG−**I** and ST-PHPMA−**I** to inhibit cathepsin K activity in synovial fibroblasts was also evaluated. Both polymer-bound inhibitors were internalized by endocytosis and were ultimately trafficked to the lysosomal compartment. ST-PHPMA−**I** was internalized faster than mPEG−**I**. The inhibitory activity in the synovial fibroblast assay correlated with the rate of internalization.

Cathepsin K, a 24 kDa cysteine protease of the papain superfamily, was first discovered in a rabbit osteoclast cDNA library and named OC-2 (*1*). The human equivalent of the protein was subsequently cloned by several groups and named cathepsin O (*2*), K (*3*), X (*4*), and O2 (*5*). By NCIUB recommendation, the protease is now designated cathepsin K. It shares the highest homology in DNA and amino acid sequence to cathepsins L and S (*5*).

In osteoclasts, cathepsin K is expressed at high level, while cathepsins B, L, and S are expressed at relatively low or undetectable levels (*1*, *5*−*7*). Deficiency of cathepsin K activity in osteoclasts induces pycnodysostosis, a rare inherited disorder with an osteopetrotic phenotype (*8*, *9*). Specific inhibition of cathepsin K expression with antisense olignucleotides has been shown to produce a 40−50% reduction in bone resorption (*10*). Cathepsin K is the only known mammalian cysteine protease capable of cleaving native type I collagen in its triple helix region (*11*, *12*). These findings clearly demonstrate the unique physiological role of this enzyme in organic matrix degradation during the bone resorption process. Recently, cathepsin K has also been shown to be able to cleave native type II collagen (*11*, *13*). The expression of cathepsin K in rheumatoid arthritis-derived synovial fibroblasts was observed and correlated with the severity of the disease (*14*). Such reports suggested the involvement of cathepsin K in cartilage breakdown in rheumatoid arthritis patients.

As a potential therapeutic target for the treatment of osteoporosis and rheumatoid arthritis, successful inhibition of cathepsin K may contribute to an understanding and final cure of these diseases. Natural inhibitors of cysteine proteases (including cathepsin K), such as cystatins (*15*) and prodomains of the zymogens (*16*, *17*), have been well studied and understood. Many low-molecular-weight cathepsin K

† This research was supported in part by NIH Grant EB00251 (to D.W., M.P., P.K., and J.K.) and by NIH Grant AR46182 and the Biomedical Science Grant from the Arthritis Foundation (to W.L. and D.B.).

* Corresponding author. Address: University of Utah, Department of Pharmaceutics and Pharmaceutical Chemistry, 30 S 2000 E Rm. 301, Salt Lake City UT 84112. Phone: + 801-581-4532. Fax: + 801-581-3674. E-mail: Jindrich.Kopecek@m.cc.utah.edu.

‡ Department of Pharmaceutics and Pharmaceutical Chemistry/CCCD, University of Utah.

§ These authors contributed equally to this work.

|| Permanent address: Institute of Macromolecular Chemistry, Academy of Sciences of the Czech Republic, Prague.

⊥ Department of Human Genetics, Mount Sinai School of Medicine.

Department of Bioengineering, University of Utah.

10.1021/bi0257080 CCC: $22.00
Published on Web 06/20/2002

inhibitors have been synthesized and investigated extensively as well (*18*, *19*).

Several challenges are faced by the possible clinical applications of synthetic cathepsin K inhibitors. Oral bioavailability is one of the critical limitations of inhibitors, which target chronic diseases (*20*). Given the proteolytic susceptibility of peptide inhibitors, peptidomimetic replacement has been considered to improve their oral bioavailability (*21*−*23*). However, data on biodistribution, in vivo stability and side effects after the administration of cathepsin K inhibitors are limited.

The localization and activation of cathepsin K has been investigated using cytochemical and immunohistochemical assays (*24*, *25*). In osteoclasts, cathepsin K was found to be expressed and processed intracellularly prior to cell attachment and bone resorption. The activation of procathepsin K is believed to be a mainly autocatalytic process within lysosomes (*26*, *27*). Once resorption started, a high level of cathepsin K was observed in both the resorption lacuna and the intracellular vesicles. In the osteoclasts of patients with cathepsin K deficiency, undigested collagen fibers were observed deposited within lysosomes, which implied the possible participation of cathepsin K in the terminal breakdown of collagen fibers during transcytotic transport of the bone resorption products (*28*). Recently, the expression of cathepsin K in rheumatoid arthritis-derived synovial fibroblasts was found to be mainly in the lysosomal compartment. Specific inhibition of cathepsin K prevents the intracellular degradation of collagen, leading to an accumulation of undigested fibers within subcellullar compartments (most likely lysosomes) (*14*). Theoretically, these experimental observations suggest that lysosomes represent an ideal subcellular target for the delivery of cathepsin K inhibitors.

Scheme 1: Synthesis of Inhibitor **I**

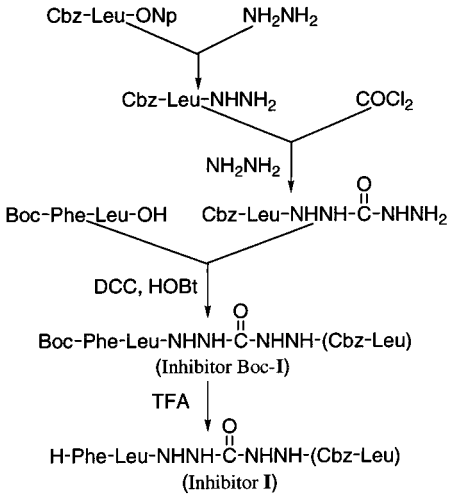

The subcellular location of cathepsin K suggests the potential for the development of a new class of cathepsin K inhibitor-conjugates of low-molecular-weight inhibitors and water-soluble polymeric carriers. Attachment of low-molecular-weight compounds, e.g., anticancer drugs, to macromolecules renders them lysosomotropic (*29*). Macromolecular therapeutics have been successfully applied to cancer chemotherapy (*30*), with one conjugate approved for clinical use in Japan (*31*) and several other conjugates in clinical trials (*32*). Therefore, conjugation to water-soluble polymers will result in internalization of cathepsin K inhibitors via the endocytic pathway (for study of endocytosis in osteoclasts, see ref *33*) and bring them into contact with the target enzyme. Incorporation of bone targeting moieties into the cathepsin K inhibitor−polymer conjugates may greatly enhance drug accumulation in hard tissues (*34*, *35*) and prevent nonspecific inhibition of cathepsin K activity in other organs, such as ovary. In addition, the enhanced vascular permeability of rheumatoid arthritis patients may result in enhanced accumulation of the conjugates in arthritis joints (*36*, *37*). Other advantages of polymer conjugation may include increased intravascular half-time and improved water solubility of hydrophobic inhibitors.

To test the hypothesis that attachment of cathepsin K inhibitors to macromolecular carriers would benefit the design of new effective inhibitors, we must answer critical questions. Will the conjugated inhibitors retain inhibition activity? If so, how would the structure of the conjugates influence their activity?

To this end, the potent selective cathepsin K inhibitor of 1,5-bis(Cbz−Leu) carbohydrazide (*38*), was modified in the present study. This was accomplished by replacing one Cbz group of the inhibitor with a phenylalanine to produce 1-(*N*-benzyloxycarbonylleucyl)-5-(phenylalanylleucyl) carbohydrazide (inhibitor **I**, Scheme 1). Inhibitor **I** was conjugated to the chain termini of two water-soluble polymers {α-methoxy poly(ethylene glycol), abbreviated as mPEG−**I**; semitelechelic poly[*N*-(2-hydroxypropyl)methacrylamide], abbreviated as ST-PHPMA−**I**}. The conjugation of inhibitor **I** to *N*-(2-hydroxypropyl)methacrylamide (HPMA) copolymer side chains was accomplished via either a Gly−Gly spacer (PHPMA−GG−**I**) or with no spacer between **I** and the copolymer backbone (PHPMA−**I**). The potency and

[1] Abbreviations: AIBN, 2,2′-azobisisobutyronitrile; Boc_2O, di(*tert*-butyl)-dicarbonate; Cbz−Leu−ONp, benzyloxycarbonyl-L-leucine *p*-nitrophenyl ester; Cbz−Phe−Arg−AMC, 7-amino-4-methylcoumarin, benzyloxycarbonyl-L-phenylalanyl-L-arginine amide; Cbz-Gly-Pro-Arg-MβNA, benzyloxycarbonyl-glycyl-L-prolinyl-L-arginyl-4-methoxy-β-naphthylamide; DCC, dicyclohexylcarbodiimide; DCU, dicyclohexyl urea; DIEA, diisopropylethylamine; DMF, *N*,*N*′-dimethyl formamide; DMSO, dimethyl sulfoxide; DTT, D,L-dithiothreitol; E-64, L-*trans*-3-carboxyoxiran-2-carbonyl-L-leucylagmatine; EDC, 1-ethyl-3-(3-dimethylaminopropyl)carbodiimide; FPLC, fast protein liquid chromatography; FITC, fluorescein isothiocyanate; HOBt, 1-hydroxybenzotriazole; HOSu, 1-hydroxysuccinimide; HPMA, *N*-(2-hydroxypropyl)methacrylamide; **I**, 1-(*N*-benzyloxycarbonylleucyl)-5-(phenylalanylleucyl) carbohydrazide; MA−GG−ONp, *N*-methacryloylglycylglycine *p*-nitrophenyl ester; MA−Phe−Leu−OH, *N*-methacryloylphenylanalanylleucine; mPEG−**I**, conjugate of **I** and mPEG2000; mPEG−FITC, conjugate of FITC and mPEG2000; M_n, number average molecular weight; MPA, mercaptopropionic acid; mPEG, poly(ethylene glycol) methyl ether; M_w, weight average molecular weight; MWD, molecular weight distribution; −ONp, *p*-nitrophenyl ester; OPA, phthalic dicarboxaldehyde; −OSu, *N*-hydroxysuccinimide ester; PHPMA, poly[*N*-(2-hydroxypropyl)methacrylamide]; P-GG-ONp, poly(*N*-(2-hydroxypropyl)-methacrylamide-*co*-*N*-methacryloylglycylglycine *p*-nitrophenyl ester); P−, PHPMA polymer backbone; PHPMA−GG−**I**, conjugate of **I** to PHPMA side chain via Gly−Gly spacer; PHPMA−**I**, conjugate of **I** to PHPMA side chain with no spacer; RFU, relative fluorescence unit; SI, stoichiometry of inhibition; SEC, size-exclusion chromatography; ST-PHPMA−COOH, semitelechelic poly[*N*-(2-hydroxypropyl)methacrylamide] having a −COOH terminus; ST-PHPMA−COOSu, semitelechelic poly[*N*-(2-hydroxypropyl)methacrylamide] having a *N*-hydroxysuccinimide ester terminus; ST-PHPMA−**I**, conjugate of **I** and ST-PHPMA−COOH; ST-PHPMA−FITC, conjugate of FITC and ST-PHPMA−COOH; TFA, trifluoroacetic acid; TNBS, 2,4,6-trinitrobenzenesulfonic acid. If not specified, all amino acids except glycine were of L configuration.

selectivity of inhibitor **I**−polymer conjugates against cathepsins K, B, L, and papain were evaluated with enzyme assays. The differences among these conjugates were related to their structures. Furthermore, the cathepsin K inhibitory activity and subcellular localization of two of the most potent conjugates were evaluated on a human primary synovial fibroblast cell culture.

EXPERIMENTAL PROCEDURES

Materials. Recombinant human cathepsin K (*6*), *N*-(2-hydroxypropyl)methacrylamide (HPMA) (*39*), and *N*-methacryloylglycylglycine *p*-nitrophenyl ester (MA−GG−ONp) (*40*) were prepared as described previously. Papain, bovine spleen cathepsin B, E-64, D,L-dithiothreitol (DTT), and dimethyl sulfoxide (DMSO) were purchased from Sigma (St. Louis, MO). Cbz−Phe−Arg−AMC (7-amino-4-methylcoumarin, benzyloxycarbonyl−L-phenylalanyl−L-arginine amide) was obtained from Bachem Bioscience Inc. (King of Prussia, PA). Cbz−Gly−Pro−Arg−MβNA (Benzyloxycarbonyl−glycyl−L-prolinyl−L-arginyl−4-methoxy-β-naphthylamide) was from Bachem Inc (Bubendorf, Switzerland). Human liver cathepsin L was purchased from Enzyme Systems Products (Livermore, CA). If not specified, all other reagents and solvents were purchased from Aldrich (Milwaukee, WI).

Methods. All polymers and inhibitor conjugates were characterized by size exclusion chromatography (SEC) using the ÄKTA FPLC system (Amersham Pharmacia Biotech) equipped with UV and RI detectors. SEC measurements were carried out on Superdex 75 or Superose 6 columns (HR 10/30) with PBS (pH 7.3) as the eluent. The average molecular weights of the polymers were calculated by calibrations using PHPMA or mPEG standards.

^{1}H NMR spectra of all synthesized compounds were recorded on a Varian Unity 500 MHz NMR spectrometer. The solvent peak was used for reference (d_6-DMSO, 2.49 ppm).

Mass spectra of all synthesized compounds were obtained using a Finnigan LCQ DECA Mass Spectrometer interfaced to an ESI source.

To determine the content of inhibitor **I**, we performed amino acid analyses of the inhibitor−polymer conjugates as follows. Fully hydrolyzed and OPA-derivatized samples (0.02 mL) were injected to a VARIAN C18 (Microsorb MV 300 Å, 250 × 4.6 mm) column at a flow rate of 1 mL/min. The elution signal was monitored with a Waters 474 Scanning Fluorescence Detector (excitation 330 nm, emission 420 nm). A gradient program was used with solvent A (0.05 M sodium acetate containing 25 mL of acetonitrile in 1 L, pH adjusted to 6 with acetic acid) and solvent B (4.1 g of sodium acetate in 300 mL water mixed with 700 mL of methanol). The gradient was programmed to start at 30% B, which increased to 80% over 42 min (hold for 10 min) and then decreased to 30% in 5 min (hold for 5 min). The amount of **I** was calculated by calibration with standard L-Phe and L-Leu.

*Synthesis of Inhibitor **I**.* The inhibitor was synthesized according to a method reported previously (*38*, *41*) with modifications. The synthetic method is depicted in Scheme 1 and described in detail below.

Cbz−Leu−NHNH$_2$. Cbz−Leu−ONp (3 g, 7.8 mmol) was dissolved in dioxane (10 mL) and added dropwise into hydrazine hydrate (1 mL, 20 mmol, in 15 mL dioxane). Orange precipitate (hydrazinium 4-nitrophenolate) was removed by filtration. 1,4-Dioxane was evaporated, and the solid residue was recrystallized from ethanol−diethyl ether with one drop of HCl (37%). The yield was 1.5 g (4.8 mmol, 62%). mp 159−160 °C.

Cbz−Leu−NHNHCONHNH$_2$. Cbz−Leu−NHNH$_2$ (1.5 g, 4.8 mmol) and phosgene (20% in toluene, 30 mL, 60 mmol) was refluxed in toluene for 4 h. The intermediate was obtained by evaporation of the solvent and used for the next reaction step without purification. TLC revealed one spot (silica gel, chloroform:ethanol 6:1, $R_f = 0.6$, UV detection). The intermediate (4.8 mmol) was dissolved in absolute ethanol (5 mL) and dropped into hydrazine hydrate (1 mL, 20 mmol, in 10 mL absolute ethanol). The reaction mixture was heated to reflux for 3 h, and then the solvent was evaporated. The residue was redissolved in ethyl acetate, and the solution was washed with aqueous sodium bicarbonate to remove any residual *p*-nitrophenol from the first reaction step. The organic layer was dried over anhydrous Na_2SO_4. The product was isolated after recrystallization from ethyl acetate with a yield of 730 mg (2.16 mmol, 45%).

Boc−Phe−Leu−OH. Phe−Leu monohydrate (1.04 g, 3.5 mmol), Boc_2O (0.85 g, 3.8 mmol), and NaOH (0.152 g, 3.8 mmol) were dissolved in water (15 mL) with dioxane (15 mL) and stirred at 4 °C overnight. The solvent was evaporated. The residue was redissolved in water (20 mL) and washed with diethyl ether to remove excess of Boc_2O. The water layer was covered with ethyl acetate and carefully acidified to pH 2 with aq. $KHSO_4$. The organic extract was washed with aq. NaCl, dried over anhydrous Na_2SO_4, and filtered. The title compound was isolated as a white powder (1.3 g, 100%) after the evaporation of the solvent. mp 148 °C.

Boc−Phe−Leu−NHNHCONHNH−(Cbz−Leu) (*Boc−**I***). Boc−Phe−Leu−OH (720 mg, 1.9 mmol), DCC (392 mg, 1.9 mmol), DIEA (0.65 mL. 3.8 mmol), HOBt (0.291 mg, 1.9 mmol), and Cbz−Leu−NHNHCONHNH$_2$ (700 mg, 2 mmol) reacted in DMF (10 mL) at 4 °C for 2 days. The precipitated DCU was filtered off. DMF was evaporated under reduced pressure, and the residue was dissolved in ethyl acetate. The solution was washed with aq. $NaHCO_3$, aq. citric acid, again aq. $NaHCO_3$, and aq. NaCl. The organic layer was dried over anhydrous Na_2SO_4, filtered, and concentrated to yield 520 mg (0.75 mmol, 40%) of very soft white crystalline solid which was isolated by centrifugation. Structure was confirmed by ^{1}H NMR (500 MHz, d_6-DMSO): δ (ppm) = 0.85 (m, 12H, CH_3-Leu), 1.28 (s, 9H, Boc), 1.47 (m, 4H, Leu), 1.63 (m, 2H, Leu), 2.71 (m, 1H, β-Phe), 2.93 (m, 1H, β-Phe), 4.07 (m, 1H, α-Leu), 4.17 (m, 1H, α-Leu), 4.38 (m, 1H, α-Phe), 5.00 (s, 2H, CH_2O), 6.92 (d, 1H, NH−Boc), 7.17−7.34 (m, 10H, arom.), 7.43 (d, 1H, NH−Cbz), 7.90 (d, 1H, NH-amide), 8.16 (d, 2H, NH-carbohydrazide), 8.72 (d, 2H, NH-carbohydrazide).

H−Phe−Leu−NHNHCONHNH−(Cbz−Leu) (***I***). Boc−**I** (0.5 g, 0.72 mmol) was dissolved in trifluoroacetic acid (TFA) (5 mL, 65 mmol) with a small crystal of phenol as a scavenger. After 30 min, TFA was evaporated, the residue was redissolved in MeOH, evaporated, then dissolved in water. The solution was further washed with diethyl ether then lyophilized. Yield (400 mg, 56%). mp 180 °C. The structure was confirmed by ^{1}H NMR (500 MHz, d_6-

Scheme 2: Structure of Macromolecular Inhibitors

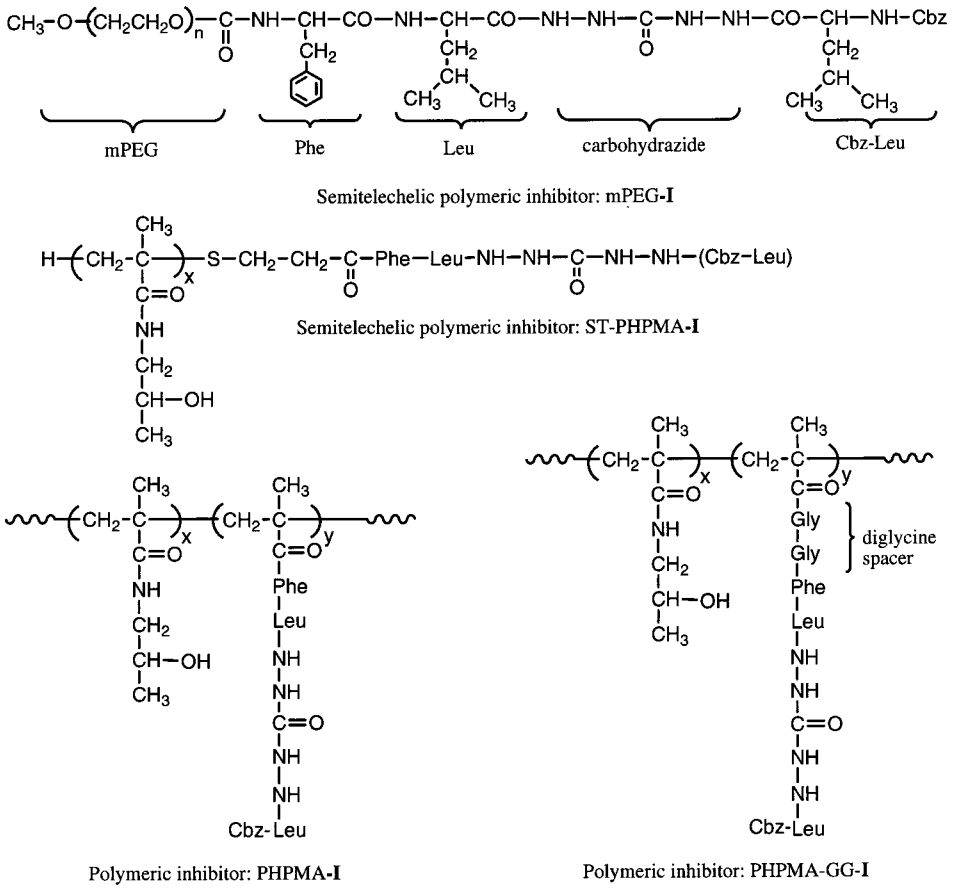

DMSO): δ (ppm) = 0.88 (m, 12H, CH_3-Leu), 1.46 (m, 4H, Leu), 1.64 (m, 2H, Leu), 2.89 (dd, 1H, β-Phe), 3.08 (dd, 1H, β-Phe), 4.06 (m, 2H, α-Leu), 4.43 (m, 1H, α-Phe), 5.00 (d, 2H, CH_2O), 7.23−7.35 (m, 10H, arom.), 7.44 (d, 1H, NH-Cbz), 8.09 (bs, 3H, NH_3^+), 8.22 (d, 2H, NH-carbohydrazide), 8.68 (d, 1H, NH-amide), 9.79 (s, 1H, NH-carbohydrazide), 9.85 (s, 1H, NH-carbohydrazide).

Synthesis of Polymer−Inhibitor Conjugates. Conjugates mPEG−**I**, ST-PHPMA−**I**, and PHPMA−GG−**I** were synthesized by the aminolysis of active esters (OSu or ONp) in the corresponding polymer precursors. PHPMA−**I** was synthesized by multistep polymer analogous reactions starting from the copolymer of HPMA and *N*-methacryloylphenylanalanylleucine (MA−Phe−Leu). The structures of the conjugates were depicted in Scheme 2, and the syntheses of these conjugates are described in detail as follows.

*Conjugate mPEG−**I***. The terminal hydroxy group of mPEG (M_n = 2000, 6.3 g, 3.15 mmol) was activated by phosgene (20% in toluene, 30 mmol) overnight. After evaporation of the toluene and phosgene, the residue was redissolved in methylene chloride. HOSu (0.4 g, 3.5 mmol) was added into the solution, followed by DIEA (450 mg, 3.5 mmol). After 2 h at 25 °C, the solution was concentrated, and the crude product was precipitated with diethyl ether, yielding 7 g of white polymer (stored at −18 °C). The activated mPEG (173 mg, 0.08 mmol active ester) and **I** (71 mg, 0.1 mmol) were dissolved in DMF (3 mL), and DIEA (0.03 mL, 0.3 mmol) was added in 2 portions. After 8 h at 25 °C, the solvent was evaporated. Residue was dissolved in methylene chloride and washed with aq. NaCl. Methylene chloride was evaporated, and the product was purified, first on a Sephadex LH-20 column with MeOH as the eluent, then on a Superdex 75 (prep.) column to remove any traces of free **I**. The polymer fraction was dialyzed (MW cutoff 1000 Da) and lyophilized to obtain 170 mg (80%) of purified conjugate mPEG−**I** used in enzyme study. The content of **I** in the final purified conjugate was determined by amino acid analysis.

*Conjugate ST-PHPMA−**I***. ST-PHPMA−COOH and ST-PHPMA−COOSu were prepared as reported previously (*42*). ST-PHPMA−COOSu (M_n = 5400, 50 mg, [-OSu] = 9.34×10^{-6} mol) and **I** (8.6 mg, 1.21×10^{-5} mol) were mixed in DMF (0.5 mL), followed by addition of DIEA (6 μL, 3.7×10^{-5} mol). The reaction mixture was stirred overnight at 25 °C, then diluted with water (10 mL), and dialyzed (MW cutoff 1000 Da). The lyophilized product was further purified with a procedure similar to the one described for mPEG−**I**. About 51 mg (93%) of the final purified conjugate ST-PHPMA−**I** was obtained and used in enzyme study. The content of **I** in the conjugate was determined by amino acid analysis.

*Conjugate PHPMA−GG−**I***. P−GG−ONp was prepared as reported previously (*40*). It (M_n = 15000, 20 mg, [−ONp] = 7.3×10^{-6} mol) was mixed with **I** (5.2 mg, 5.84×10^{-6} mol) in DMSO (0.5 mL), followed by addition of DIEA (12.8 μL, 7.3×10^{-5} mol). It was stirred overnight at 25 °C. The resulting solution was further diluted into water (10 mL) and then dialyzed against water for 1 day (MW cutoff 1000 Da). A purification procedure similar to the one described for mPEG−**I** was used to remove remaining *p*-nitrophenol and

any possible free **I**. The final purified product was lyophilized to yield 21 mg (88%) of conjugate PHPMA−GG−**I**. The content of **I** in the conjugates was determined by amino acid analysis.

*Conjugate PHPMA−**I***. HPMA (0.95 g, 6.63×10^{-3} mol, 95 mol %), MA−Phe−Leu−OH (0.121 g, 3.5×10^{-4} mol, 5 mol %), MPA (6.82×10^{-5} mol), and AIBN (0.052 g) were dissolved in acetone (10 mL) and copolymerized for 24 h to yield 0.8 g of poly[HPMA-*co*-MA−Phe−Leu−OH]. The copolymer (100 mg, 3.11×10^{-5} mol, COOH) and carbohydrazide (283 mg, 3.11×10^{-3} mol) were dissolved in H_2O. EDC (0.596 g, 3.11×10^{-3} mol) and HOBt (0.42 g, 3.11×10^{-3} mol) were dissolved in DMF and H_2O mixture (5 mL + 2.5 mL), and this solution was added into a polymer solution. The mixture was stirred at 4 °C for 4 h and then 25 °C for 24 h. The solution was dialyzed against H_2O (pH 2, adjusted with 6M HCl) for 24 h and then against H_2O (pH 7) for 12 h. It was lyophilized to yield 106 mg of P−Phe−Leu−NHNHCONHNH$_2$. With TNBS assay, the amount of NH_2NH- side chains was determined as 1.94×10^{-4} mol/g. The hydrazide containing polymer (50 mg, NH_2-NH− = 9.75×10^{-6} mol) and TEA (56 mL, 3.89×10^{-4} mol) was dissolved in DMF (1 mL). Cbz−Leu−ONp (75.15 mg, 1.95×10^{-4} mol) was dissolved in DMF (0.5 mL). The two solutions were mixed and stirred at 25 °C for 12 h. The solvent was removed, and the solid was dissolved in MeOH. A purification procedure similar to the one described for mPEG−**I** was used to remove any remaining low-molecular-weight compound. Finally, 50 mg (93%) of lyophilized pure conjugate PHPMA−**I** was obtained for enzyme study. The amount of unreacted NH_2NH- was determined with TNBS assay (less than 2% left).

Synthesis of Polymer−FITC Conjugates. Fluorescein cadaverine was conjugated to mPEG and ST-PHPMA following a similar strategy as the synthesis of mPEG−**I** and ST-PHPMA−**I**. The same mPEG and ST-PHPMA polymeric precursors were used. They were purified with a similar procedure as well.

Enzyme Assays. Standard enzyme assay and inhibition studies were performed at 37 °C in acetate buffer (0.1 M, pH 5.6) containing 2.5 mM EDTA and 0.03% Brij35 (except the case of papain, in which 0.1 M phosphate buffer with pH 6.5 was used instead). Cbz−Phe−Arg−AMC was used as the substrate in all cases. AMC released was monitored with a SPECTRAmax, GEMINI XS microplate spectrofluorometer system (excitation/emission 380/450 nm, cutoff 420 nm). Automix (3 s) was done prior to each measurement. All curve fitting was performed using Kaleida Graph 3.09 software.

The concentrations of active protein in all enzymes that used in this study were determined by titration with E-64 (*43*). The kinetic constants V_{max} and K_m were obtained by nonlinear regression analysis, and k_{cat} and k_{cat}/K_m were calculated thereafter.

Enzyme inactivation assays were performed in 96-well plates. Enzyme and DTT (2.5 mM, final) were mixed and preincubated for 5 min at 37 °C. Premixed substrate and inhibitor were then added to initiate the reaction. The substrate concentration used was equivalent to K_m (final) for each enzyme. Inhibitor concentrations used were adjusted according to potency. The final enzyme concentration was 0.5 nM in all cases. All progress curves were fitted to the equation

$$[\mathrm{AMC}] = \nu_{ss}t + (\nu_0 - \nu_{ss})[1 - \exp(-k_{obs}t)]/k_{obs} + A_0 \quad (1)$$

where ν_0 is the initial reaction velocity, ν_{ss} is the final steady-state rate, A_0 is the background fluorescence, and k_{obs} is the rate of inactivation. By relating k_{obs} with inhibitor final concentration [I], an apparent second-order rate constant k_{obs}/[I] can be obtained to evaluate the selectivity and potency of the inhibitors.

Assuming the inhibitors are purely competitive, an apparent inhibition constant ($K_{i,app}$) can be obtained for the formation of the initial reversible enzyme−inhibitor complex prior to inactivation:

$$\nu_0 = V_{max}[S]/(K_m(1 + [I]/K_{i,app}) + [S]) \quad (2)$$

Since the inactivation is done with $[S] = K_m$, eq 2 can be reduced into

$$\nu_0 = V_{max}/(2 + [I]/K_{i,app}) \quad (3)$$

By relating ν_0 with different concentrations of inhibitor, $K_{i,app}$ can be obtained. This kinetic treatment and its application to cathepsin K inhibitors have been reported previously (*44*, *45*).

Stoichiometry of inhibition (SI) for the interaction between all inhibitors synthesized and cathepsin K and papain was determined as follows. Fixed amounts of enzymes (0.5 nM) were activated with DTT and incubated with different concentrations of inhibitors (based on the potency of the inhibitors) for 30−60 min. The substrate (Cbz−Phe−Arg−AMC) was then added to start the reaction. The observed residual enzyme activity was plotted versus inhibitor concentration, and the SI values, which resulted in complete enzyme inhibition, were calculated.

Inhibition of Cathepsin K in Synovial Fibroblasts. The cathepsin K inhibition activities of the low-molecular-weight inhibitors (**I** and Boc−**I**) and the inhibitor-polymer conjugates (mPEG−**I** and ST-PHPMA−**I**) were evaluated in primary human synovial fibroblast cultures using an in situ fluorogenic substrate, Cbz−Gly−Pro−Arg−MβNA, as described previously (*24*). Low-molecular-weight inhibitors were tested at one concentration (1 μM), while both macromolecular inhibitors were tested at two concentrations (1 and 10 μM). Briefly, the inhibitor treated synovial fibroblasts were incubated with a mixture of 1 mg/mL Cbz-Gly-Pro-Arg-MβNA, 1 mM 5-nitrosalicylaldehyde, 1 mM DTT, 2.7 mM L-cysteine, 0.25 mM EDTA in 100 mM acetate buffer (pH 5.5) for 30 min. The generation of the insoluble fluorescent product was monitored using a Nikon Eclipse E800 fluorescence microscope (excitation 440−500 nm and emission above 510 nm). To address the uptake of polymer into the cells, we used polymer-FITC conjugates. The cells were incubated with the conjugates (100 μM) in 5% CO_2 incubator at 37 °C for 5 h. After washing three times with PBS, the intracellular fluorescent signal was detected by fluorescence microscopy.

RESULTS

*Synthesis and Characterization of **I** and Its Conjugates with Water-Soluble Polymers.* Inhibitor **I** was synthesized

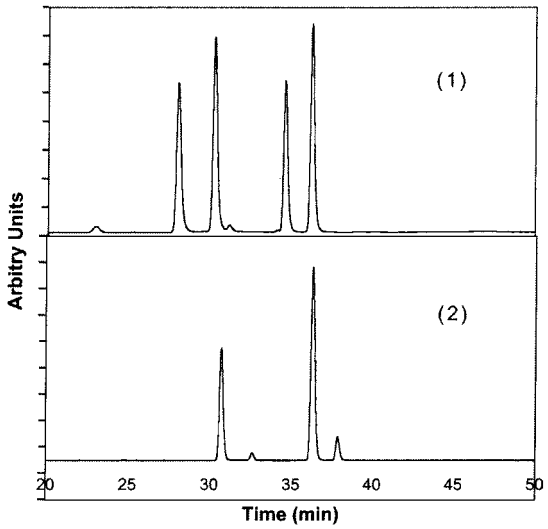

FIGURE 1: HPLC chromatograms of amino acids (derivatized with phthalic dicarboxaldehyde and thio glucose). (panel 1) Calibration: 27.99 (D-Phe), 30.20 (L-Phe), 34.56 (D-Leu), and 36.20 min (L-Leu). (panel 2) Hydrolyzed conjugate mPEG−**I**: 30.74 (L-Phe), 32.64 (unknown), 36.35 (L-Leu), and 37.9 min (unknown).

Table 1: Characterization of Inhibitors

inhibitor	molecular weight	content of inhibitor **I**[a]	number of **I** per polymer chain
I	597.71	–	–
Boc−**I**	697.85	–	–
mPEG−**I**	2700[b]	3.60×10^{-4} mol/g	1.0
ST-PHPMA−**I**	4230[b]	1.44×10^{-4} mol/g	0.6
PHPMA-GG−**I**	7700[b]	1.49×10^{-4} mol/g	1.1
PHPMA−**I**	15500[b]	1.91×10^{-4} mol/g	2.9

[a] Determined by amino acid analysis, except PHPMA−**I**, which was analyzed by TNBS assay. [b] Number average molecular weights were determined by SEC.

at high yield using the procedure described in Scheme 1. In salt form ($-NH_3^+ \cdot CF_3COO^-$), **I** was water-soluble. Racemization was not observed in **I** and its polymer conjugates. In a typical HPLC chromatogram of hydrolyzed conjugate mPEG−**I** (panel 2 in Figure 1), no peak can be assigned to D-Phe or D-Leu according to the calibration (panel 1 in Figure 1). Peaks with retention times at 30.74 and 36.35 min in panel 2 can be assigned to L-Phe and L-Leu, respectively. Their ratio was close to 0.5, which is in a good agreement with the composition of **I**. From this, it can be concluded that intact **I** has been conjugated to the polymer. Two very small peaks at 32.6 and 37.9 min in panel 2 may be assigned to unknown impurities from the OPA derivatization of hydrolyzed mPEG−**I**. The final calculation of inhibitor content in all conjugates was based on L-amino acid peak-areas.

Synthesized conjugates were carefully purified by column chromatography and dialysis. Their purity was confirmed by their respective SEC profiles, which indicated the absence of low-molecular-weight compounds trapped physically in the conjugates. The molecular weight and inhibitor content of the conjugates are summarized in Table 1. As one can see from the data, blank polymer with no **I** attachment was abundant in conjugate ST-PHPMA−**I** (about 40%), since the average number of **I** per polymer chain in the conjugate is only 0.6. Although all other conjugates had on average more than one **I** moiety attached to each polymer chain, the presence of unsubstituted polymer chains is possible. The concentration of polymeric inhibitors in enzyme study was calculated based on the content of **I**.

Table 2: Kinetic Parameters for Enzymes Using Cbz−Phe−Arg−AMC as the Substrate[a]

enzyme	k_{cat} (s^{-1})	K_m (μM)	k_{cat}/K_m ($M^{-1}\,s^{-1}$)
cathepsin K	19.3	39.2	492 000
cathepsin L	16.5	5.87	2 810 000
cathepsin B	48.4	202	240 000
papain	21.1	76.4	276 000

[a] All data were obtained with platereader assay.

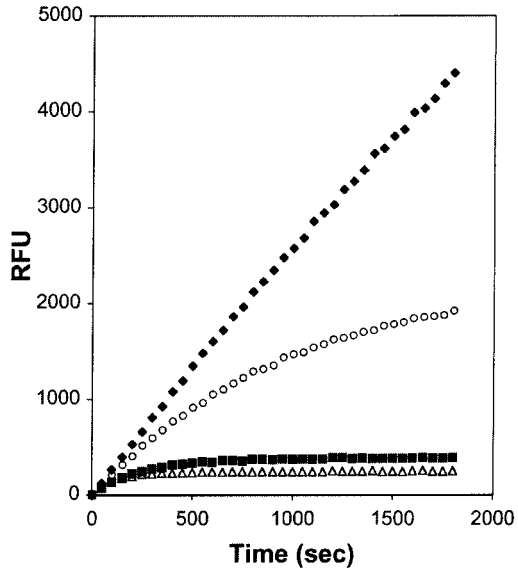

FIGURE 2: Inhibition progress curves of cathepsin K-catalyzed hydrolysis of Cbz−Phe−Arg−AMC in the presence of the inhibitor Boc−**I** at 37 °C in acetate buffer (0.1 M, pH = 5.6) containing 2.5 mM EDTA, 2.5 mM DTT, and 0.03% Brij35. The substrate concentration was 6.72×10^{-5} M. The final concentration of cathepsin K was 0.5 nM. The following inhibitor concentrations were used: 0 (◆), 1.5 (○), 7.5 (■), and 15 nM (△). The fluorescence generated (released AMC) was monitored with a microplate spectrofluorometer (excitation/emission 380/450 nm, cutoff 420 nm). RFU, relative fluorescence unit.

Kinetic Parameters for Cathepsins K, L, B, and Papain Using Cbz−Phe−Arg−AMC as Substrate. Kinetic parameters such as k_{cat}, K_m, and k_{cat}/K_m determined with platereader assay are shown in Table 2. All k_{cat}/K_m values for the tested enzymes with Cbz-Phe-Arg-AMC as the substrate are in the same range as previously published data, indicating the substrate is better for cathepsin L than for the other three enzymes (*6*, *46*). The K_m values for cathepsin K and papain were higher than some of the published data (*6*, *47*); this could be attributed to a higher amount of DMSO (5 v/v%) used in this study (*48*).

*Inhibition Activity of Inhibitors **I** and Boc−**I** Against Cathepsins K, L, B, and Papain.* Both **I** and its Boc protected derivative possessed inhibitory activities similar to unmodified 1,5-bis(Cbz−Leu) carbohydrazide. The effect of various concentrations of Boc−**I** on the rate of hydrolysis of the fluorescent substrate Cbz−Phe−Arg−AMC by cathepsin K is shown in Figure 2. The nonlinear character of these progress curves indicated that Boc−**I** is a time-dependent inhibitor of the enzyme like 1,5-bis(Cbz−Leu) carbohydrazide and **I**. These inhibition curves were fit into eq 1 to determine the inactivation rate k_{obs} and initial hydrolysis

Table 3: Inhibition of Papain Superfamily Members by Compounds **I** and Boc−**I**[a]

	I		Boc−**I**	
	k_{obs}/[I] (M^{-1} s^{-1})	$K_{i,app}$ (nM)	k_{obs}/[I] (M^{-1} s^{-1})	$K_{i,app}$ (nM)
cat K	1.3×10^6 (3.5×10^4)	9.7	5.9×10^5 (1.2×10^4)	6.0
cat L	4.1×10^4 (5.9×10^3)	1.2×10^2	1.1×10^4 (5.6×10^2)	*b*
cat B	1.8×10^2 (36.3)	5.1×10^3	2.2×10^4 (4.3×10^3)	5.1×10^2
papain	2.7×10^3 (108)	2.3×10^3	3.9×10^3 (63.5)	1.2×10^3

[a] Errors calculated from curve fitting are shown in parentheses. [b] Initial hydrolysis rates did not change enough to determine $K_{i,app}$.

Table 4: Inhibition of Papain Superfamily Members by Conjugates mPEG−**I**, ST-PHPMA−**I**, PHPMA−GG−**I**, and PHPMA−**I**[a]

	mPEG−**I**		ST-PHPMA−**I**		PHPMA−GG−**I**		PHPMA−**I**	
	k_{obs}/[I] (M^{-1} s^{-1})	$K_{i,app}$ (nM)	k_{obs}/[I] (M^{-1} s^{-1})	$K_{i,app}$ (nM)	k_{obs}/[I] (M^{-1} s^{-1})	$K_{i,app}$ (nM)	k_{obs}/[I] (M^{-1} s^{-1})	$K_{i,app}$ (nM)
cat K	5.5×10^5 (3.1×10^4)	6.6	4.5×10^5 (1.5×10^4)	11.3	2.9×10^4 (5.7×10^2)	392	3.4×10^4 (6.2×10^2)	270
cat L	3.1×10^4 (1700)	*b*	1.2×10^4 (750)	*b*	6.3×10^2 (31)	*b*	1.3×10^3 (66.6)	1.2×10^4
cat B	3.9×10^3 (207)	1.6×10^3	2.8×10^3 (86.6)	2.7×10^3	5.7×10^2 (101)	6.9×10^3	5.6×10^1 (1.7)	1.1×10^5
papain	3.1×10^3 (95.2)	2.4×10^3	2.7×10^3 (75.7)	1.9×10^3	3.4×10^2 (20.9)	1.2×10^4	2.5×10^2 (10.2)	1.3×10^4

[a] Errors calculated from curve fitting are shown in parentheses; concentrations of macromolecular inhibitors are expressed as **I** equivalents. [b] Initial hydrolysis rates did not change enough to determine $K_{i,app}$.

velocity. Analysis of initial rates of substrate hydrolysis as a function of inhibitor concentration yielded an apparent inhibition constant ($K_{i,app}$) for a reversible association of the inhibitor with cathepsin K prior to the time-dependent step.

All the enzymes tested showed similar time-dependent inhibition progress curves as those depicted in Figure 2. Second-order rate constants for inhibition k_{obs}/[I] and $K_{i,app}$ of **I** and Boc−**I** against cathepsins K, L, B and papain are summarized in Table 3. Both Boc−**I** and **I** showed potent inactivation of cathepsin K. Their $K_{i,app}$ values were in the nanomolar range, which indicated a strong inhibition of the initial rate of substrate hydrolysis. A high value for the second-order rate constant k_{obs}/[I] of the two inhibitors (**I** and Boc−**I**; $\sim 10^6$ M^{-1} s^{-1}) suggests that they are potent time-dependent inhibitors of cathepsin K, as well. These values are very close to those found for 1,5-bis(Cbz−Leu) carbohydrazide, as reported previously (*45*).

The high selectivity of Boc−**I** and **I** toward cathepsin K was demonstrated when they were tested for inhibitory activity toward other members of papain superfamily. Cathepsin L was inactivated by compounds **I** and Boc−**I** 30 to 50-fold less efficiently than cathepsin K, which was reflected by the value of k_{obs}/[I] and $K_{i,app}$ (Table 3). Inhibition parameters determined for cathepsin B and papain were about 2−4 orders of magnitude lower than those found for cathepsin K. This is consistent with the fact that cathepsin L has the highest DNA and amino acid sequence homology to cathepsin K among the papain superfamily (*6*).

The presence of NH_2 in **I** did not reduce its inhibition activity against cathepsin K. In fact, inhibitor **I** showed a higher k_{obs}/[I] than that of Boc−**I** and was close to the value of a similar molecule reported previously (*45*). Interestingly, the influence of Boc protection over NH_3^+ in **I** was observed only during the inhibition of cathepsin B, in which case, the k_{obs}/[I] value of Boc−**I** was about 2 orders of magnitude higher than that for **I**.

Inhibition Activity of Conjugates mPEG−I, ST-PHPMA−I, PHPMA−GG−I, and PHPMA−I Against Cathepsin K, L, B, and Papain. Like inhibitor **I**, conjugate mPEG−**I** was a time-dependent inhibitor of cathepsin K, typically producing nonlinear progress curves as those shown in Figure 2. This feature was shared by the other conjugates ST-PHPMA−**I**, PHPMA−GG−**I**, and PHPMA−**I** as well. Similar patterns of inhibition progress curves were observed with conjugates mPEG−**I**, ST-PHPMA−**I**, PHPMA−GG−**I**, and PHPMA−**I** when they were tested against cathepsin L, cathepsin B, and papain. With values of k_{obs}/[I] of about 5×10^5 M^{-1} s^{-1} and $K_{i,app}$ in the range of 6−11 nM, it was suggested that the inhibitory activity of conjugates mPEG−**I** and ST-PHPMA−**I** (in which **I** was attached to the polymer terminus) against cathepsin K was only slightly reduced compared to the inhibition by unbound **I** (see Table 4).

Similar values of k_{obs}/[I] and $K_{i,app}$ determined for mPEG−**I** and ST-PHPMA−**I** indicate that the different chemical compositions of each polymer did not show any apparent influence upon the inhibitory activity against cathepsin K. Their k_{obs}/[I] values against cathepsin L were 1 order of magnitude lower than the values for cathepsin K. When they were tested against cathepsin B and papain, the values were about 2 orders of magnitude lower than those with cathepsin K. Apparently, both conjugates showed similar pattern of potency and selectivity against cathepsin K as inhibitors **I** and Boc−**I**.

Both PHPMA−GG−**I** and PHPMA−**I** were relatively poor (compared to mPEG−**I** and ST-PHPMA−**I**) but selective inhibitors of cathepsin K. Their k_{obs}/[I] values (about 3×10^4 M^{-1} s^{-1}) were generally 1−2 orders of magnitude lower than those of mPEG−**I** and ST-PHPMA−**I**, while $K_{i,app}$ values were about 1−2 orders of magnitude higher. The influence of the Gly-Gly spacer was not significant and was only observed when tested against cathepsin B, in which case conjugate PHPMA−**I** (without spacer) showed about a 10 times lower k_{obs}/[I] and a 20 times higher $K_{i,app}$ than PHPMA−GG−**I** (with spacer).

Stoichiometry of inhibition (*SI*). SIs for cathepsin K and papain were determined with all inhibitors synthesized (Table 5). For cathepsin K, **I**, Boc−**I**, mPEG−**I**, and ST-PHPMA−**I** possessed SI values of about 1, while the two conjugates baring inhibitor **I** on the side chains of the polymer backbone (PHPMA−GG−**I** and PHPMA−**I**) showed slightly higher values of about 2 and 5. However, the high SI data obtained for papain indicate that all inhibitors were poor inhibitors of papain.

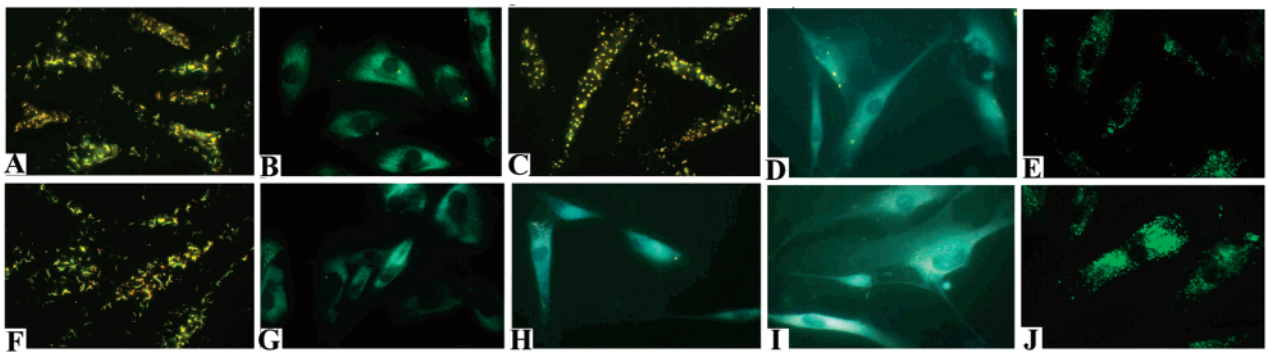

FIGURE 3: Inhibition of cathepsin K activity in human synovial fibroblasts with **I**, Boc−**I**, mPEG−**I**, and ST-PHPMA−**I**. A, no inhibitor; B, **I** (1 μM); C, mPEG−**I** (1 μM); D, mPEG−**I** (10 μM); E, mPEG−FITC (100 μM); F, no inhibitor; G, Boc−**I** (1 μM); H, ST-PHPMA−**I** (1 μM); I, ST-PHPMA−**I** (10 μM); J, ST-PHPMA−FITC (100 μM). The inhibition activities of the inhibitors and inhibitor−polymer conjugates were demonstrated by the reduction or disappearance of insoluble fluorescent product from cathepsin K hydrolysis of Cbz−Gly−Pro−Arg−MβNA (Nikon Eclipse E800, excitation 440−500 nm and emission above 510 nm). Control studies on polymer cellular entry were performed by incubating cells with mPEG−FITC and ST-PHPMA−FITC (with concentrations of 100 μM) in 5% CO_2 incubator at 37 °C for 5 h. After three washings with PBS, the intracelluar fluorescent signal was detected by fluorescent microscopy. Concentrations in parentheses refer to either **I** or FITC.

Table 5: Stoichiometry of Inhibition for Cathepsin K and Papain

inhibitor	Cathepsin K	Papain
I	1.10	11.3
Boc−**I**	0.92	221
mPEG−**I**	0.90	19.4
ST-PHPMA−**I**	0.98	20.2
PHPMA−GG−**I**	2.24	57.0
PHPMA−**I**	5.00	141

The Inhibition of Cathepsin K in Synovial Fibroblasts. The intracellular cathepsin K inhibition activities of low-molecular-weight inhibitors (**I** and Boc−**I**) and inhibitor polymer conjugates (mPEG−**I** and ST-PHPMA−**I**) were demonstrated with a fluorescent substrate cleavage assay (Figure 3) (*24*). In the absence of any inhibitor, abundant insoluble fluorescent precipitate from the hydrolysis of the cathepsin K specific substrate, Cbz−Gly−Pro−Arg−MβNA, was observed, indicating a strong lysosomal cathepsin K activity in synovial fibroblasts. Preincubation of synovial fibroblasts with 1 μM low-molecular-weight inhibitors (**I** or Boc−**I**, 30 min) could greatly decrease the intensity of insoluble fluorescent precipitate in the cells, which indicated a complete inhibition of cathepsin K activity. Differently, after preincubation with 1 μM macromolecular inhibitors (30 min), the intensity of insoluble fluorescent precipitate slightly decreased in the cells treated with mPEG−**I**, while almost no insoluble fluorescent precipitate could be observed in the cells treated with ST-PHPMA−**I**. This suggested a modest inhibition of cathepsin K by mPEG−**I** and an almost complete inhibition by ST-PHPMA−**I**. When the concentrations of macromolecular inhibitors were raised to 10 μM (30 min preincubation), complete inhibition of the Cbz−Gly−Pro−Arg−MβNA-cleaving activity in synovial fibroblasts was achieved in both cases. To demonstrate the internalization and subcellular location of the macromolecular inhibitor, we incubated mPEG−FITC and ST-PHPMA−FITC with the cells and monitored them using a fluorescence microscope. Both FITC−polymer conjugates were predominantly localized in vesicles indicative of the endosomal−lysosomal compartment. Under identical assay conditions, a stronger fluorescence intensity was observed in the cells treated with ST-PHPMA−FITC than in those treated with mPEG−FITC (Figure 3).

DISCUSSION

Modification of 1,5-Bis(Cbz−Leu) Carbohydrazide for Polymer Conjugation. Redesign of an available inhibitor may be necessary before its conjugation to polymers. When not available, an attachment site (functional group) has to be created. To minimize the impact on the inhibitory activity, the structural modification should be at a site with little influence on the formation of the enzyme−inhibitor complex

Crystallographic analysis of cathepsin K−1,5-bis(Cbz−Leu) carbohydrazide complex at 2.2 Å resolution showed that the central urea carbonyl group of the inhibitor binds to the catalytic cysteine thiol of cathepsin K. The inhibitor is bound across both the *S* and *S′* subsites of the active site. On the *S* side, Leu is bound tightly in the S_2 pocket, and the phenyl portion of Cbz appears to participate in an edge-faced $\pi-\pi$ interaction with Tyr-67. On the *S′* side, Cbz is oriented to participate in a $\pi-\pi$ interaction with Trp-184, whereas the isobutyl group is involved in a hydrophobic interaction with one face of the active site composed of Gln-21, Cys-22, and Gly-23 (*38*).

To retain the binding characteristics of the original structure, we used a phenylalanine to replace the Cbz group in 1,5-bis(Cbz−Leu) carbohydrazide. An amino group was introduced into the inhibitor structure as an attachment point for polymer conjugation (Scheme 1). This strategy was successful because the newly synthesized inhibitor **I** was as potent a selective cathepsin K inhibitor as 1,5-bis(Cbz−Leu) carbohydrazide (Table 3). In addition, Boc−**I**, which had the $-NH_2$ in **I** protected with Boc was also an effective cathepsin K inhibitor. On the basis of the results described here, neither $-NH_2$ nor Boc−NH disturbed the formation of the enzyme−inhibitor complex. However, Boc−**I** showed a much higher activity than **I** in the inhibition of cathepsin B. Hypothetically, favorable hydrophobic interaction between Boc and the enzyme active site improved binding (*49*).

Influence of Polymer Conjugation on the Activity of Inhibitors. The interactions between synthetic polymer−oligopeptide conjugates and enzymes have been studied systematically and reviewed previously (*50*). Oligopeptides with different sequence structure and length were conjugated to side chains (*51*−*54*), main chains (*55*), and chain termini

Scheme 3: Possible Structures of Polymer Conjugated **I**−cathepsin K Complex: (a) **I** Attached to Polymer Chain Termini; (b) **I** Attached to Polymer Side Chains; (c) **I** Attached to Polymer Side Chains via a Long Spacer[a]

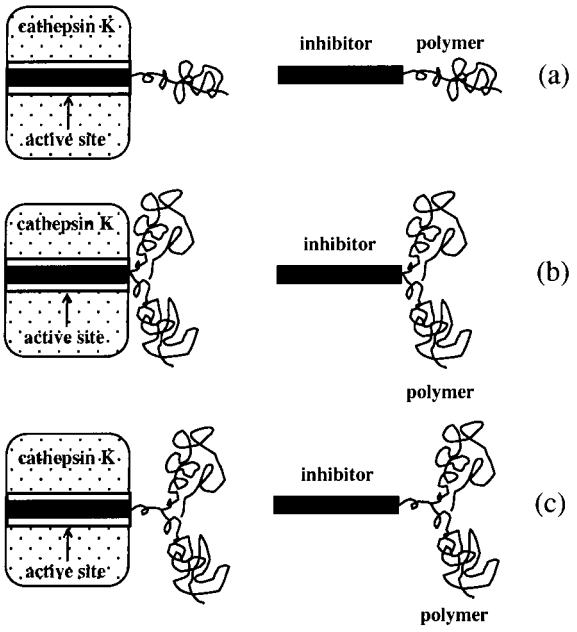

[a] The dotted area represents the body of enzyme; the white area represents the active site cleft on the enzyme surface; the black area represents the inhibitor aligned in the enzyme active site; and random coils represent water-soluble polymers.

(*55*) or were used as cross-links to join two chains (*56*−*59*) of HPMA copolymers or PEG. The degradation of polymer-bound oligopeptide substrates was evaluated with model enzymes, including trypsin (*51*), chymotrypsin (*55*, *56*, *59*), papain (*58*), and cathepsin B (*54*). The degradability of the polymer-conjugated oligopeptides may be affected by both steric and structural factors, depending on the structure and length of the oligopeptide sequences, the structure of the polymer, and mode of attachment (side chain, chain terminus, cross-link). The influence of steric hindrance from the polymer chain on the formation of the enzyme−substrate complex is often a function of the length of the incorporated oligopeptide sequence and its mode of attachment to the polymer chain (*50*).

These results may give further insight into the relationship between the structure of inhibitor−polymer conjugates and the formation of the inhibitor−target enzyme complex. Different shielding effects in the formation of inhibitor−enzyme complex posed by the conjugated polymers may impact the inhibitory activity of macromolecular inhibitors (polymer−**I** conjugates).

As the 3-D structure of 1,5-bis(Cbz−Leu) carbohydrazide aligned in the active site of cathepsin K (Protein Data Bank Id: 1AYU) shows, the 1,5-bis(Cbz−Leu) carbohydrazide spans the entire active site on the surface of cathepsin K. We hypothesize that **I** has a similar binding mode. Therefore, as shown in Scheme 3a, the conjugation of **I** to the terminus of a linear polymer via the $-NH_2$ group of Phe at the end of binding site would have little influence upon the fitting of the inhibitor. The data shown in Table 4 support this hypothesis, where both conjugates mPEG−**I** and ST-PHPMA−**I** (**I** conjugated to polymer terminus, MW < 5000) are identified as selective inhibitors of cathepsin K potent as inhibitor **I**. This is also in a good agreement with a previous report, in which the release rate of NAp from Ala−Gly−Val−Phe−NAp conjugated to the chain terminus of PEG was found to be comparable to free Ala−Gly−Val−Phe−NAp (*55*).

PEG is a water-soluble macromolecule with an expanded conformation in water (*60*), whereas PHPMA is a random coil (*61*) in aqueous solution. Higher steric hindrance to binding had been expected when **I** was conjugated to the chain terminus of ST-PHPMA, compared to mPEG conjugates. However, the results show that the steric hindrance was not significant. Probably, this is due to the existence of the 3 carbon spacer (from MPA in the synthesis of ST-PHPMA−COOH) between **I** and the PHPMA chain. The steric hindrance of the polymer backbone on the formation of the inhibitor−enzyme complex was more pronounced when **I** was conjugated to the side chains of HPMA copolymers in conjugates PHPMA−GG−**I** and PHPMA−**I**. As depicted in Scheme 3b, the formation of the inhibitor−enzyme complex may result in the distortion of the random coil conformation of the polymer backbone. Since this is not energetically favorable, it would result in a decreased inhibitory potency of conjugates PHPMA−GG−**I** and PHPMA−**I** when compared to conjugates mPEG−**I** and ST-PHPMA−**I** (Table 4). Introduction of a short rigid Gly−Gly spacer into the structure of conjugate PHPMA−GG−**I** did not alter the inhibition activity toward cathepsin K (compare conjugates PHPMA−GG−**I** and PHPMA−**I**). However, the activity of conjugate PHPMA−GG−**I** toward cathepsin B was improved.

The above analyses are in agreement with the stoichiometry of inhibition (SI) data for cathepsin K (Table 5), where both low-molecular-weight inhibitors (**I** and Boc−**I**) and semitelechelic polymer−inhibitor conjugates (mPEG−**I** and ST-PHPMA−**I**) showed a SI value of about 1, while PHPMA−GG−**I** and PHPMA−**I** demonstrated higher values of ∼2 and 5, respectively. It appears that macromolecular inhibitors where the inhibitor **I** is bound to polymer side chains (PHPMA−GG−**I** and PHPMA−**I**) are less effective because steric hindrance of the polymer chain renders the formation of the inhibitor−cathepsin K complex more difficult. The high SI values for papain (Table 5) reflect the fact that all inhibitors are poor papain inhibitors (Tables 3 and 4). Other factors contributing to the high SI values for papain may be the steric hindrance of polymeric chains (inhibitors PHPMA−GG−**I** and PHPMA−**I**) and the poor fitting of the Boc protected low-molecular-weight inhibitor (Boc−**I**) into the papain active site.

Previous data indicate that the steric hindrance can be minimized if a sufficiently long spacer is introduced between the polymer backbone and the sequence to be accommodated into the enzyme active site. For example, the binding of L-*trans*-epoxysuccinyl-leucylamido(4-amino)butane (Ep-459), a cysteine protease inhibitor, to the side chains of HPMA copolymer via a Gly−Leu spacer did not result in a decrease of its inhibitory activity toward cathepsin B or result in a change of its inhibitory activity of the intralysosomal degradation of macromolecular substrates in yolk sac tissue when compared with free (unbound) Ep-459 (*62*). The chymotrypsin catalyzed rate of cleavage of the leaving group at the termini of oligopeptide side chains attached to HPMA copolymers was strongly dependent on the length of the

oligopeptides (*51*). On the basis of these data, one may hypothesize that steric hindrance may be minimized and inhibition activity of **I** retained, if conjugation to the HPMA copolymer side chains is accomplished via longer flexible spacers (as shown in Scheme 3c).

Conjugation of **I** to side chains of HPMA copolymer via an acid cleavable spacer is another possible approach in the design of novel macromolecular cathepsin K inhibitors. Such conjugates, once transported into endosomes and/or lysosomes, would release free (low-molecular-weight) inhibitor by acid-catalyzed hydrolysis in response to the lower pH in these subcellular compartments.

Inhibition of Cathepsin K Activity in Synovial Fibroblasts. Both mPEG−**I** and ST-PHPMA−**I** were selected for the inhibition study because of their high inhibitory potency and selectivity toward cathepsin K. They both completely inhibited cathepsin K activity in synovial fibroblasts at 10 μM. However, differences in inhibitory efficacy were revealed at lower inhibitor concentrations (1 μM). Whereas the ST-PHPMA−**I** conjugate inhibited the hydrolysis of Cbz-Gly−Pro−Arg−MβNA at 1 μM concentration, the mPEG−**I** conjugate required 10 μM. Since both inhibitor−polymer conjugates shared similar k_{obs}/[I] and $K_{i,app}$ in the enzyme assay, the observed efficacy differences in the cell assay may be attributable to different internalization rates of the inhibitors. This assumption was supported by the fact that ST-PHPMA−FITC was internalized by synovial fibroblasts faster than mPEG−FITC under identical experimental conditions (Figure 3). However, since endocytosis is a concentration dependent process as well, both conjugates inhibited cathepsin K activity in the cell assay at higher inhibitor concentrations (10 μM). These data seem to suggest that PHPMA is a better carrier for cathepsin K inhibitors than PEG. As expected, both **I** and Boc−**I** can inhibit the cathepsin K activity in synovial fibroblasts at low concentration (1 μM). This reflects the fact that in an in vitro study the efficacy is being compared on the basis of extracellular concentrations; this may result in different intracellular concentrations due to differences in the mechanism of cell entry. Whereas macromolecules (polymer−inhibitor conjugates) enter cells by endocytosis, low-molecular-weigh compounds (**I** and Boc−**I**) enter cells and subcellular compartments by diffusion (*30*). Though the latter can inhibit the cathepsin K activity in cell culture experiments, systemic administration of such compounds may lead to serious side effects, such as the unwanted inhibition of cathepsin K activity in ovary, thyroid, etc. However, it could be overcome by conjugations to water-soluble polymers, which will results in numerous advantages: the possibility of introducing bone targeting moieties, passive targeting based on the enhanced permeability and retention (EPR) effect (*30*, *36*), lysosomotropism, increased intravascular half-time, and improved water solubility of hydrophobic inhibitors.

CONCLUSIONS

(a) 1-(*N*-Benzyloxycarbonylleucyl)-5-(phenylalanylleucyl) carbohydrazide (**I**) and its conjugates with ST-PHPMA, HPMA copolymers, and mPEG were synthesized and characterized.

(b) The inhibition potency of macromolecular cathepsin K inhibitors depended on the mode of inhibitor **I** attachment. Attachment to polymer chain termini resulted in minimal steric hindrance of the polymer chain on the formation of inhibitor−enzyme complex. On the other hand, attachment to side chains of HPMA copolymer resulted in steric hindrance, which led to a decrease of inhibitor potency when compared to free (unbound) inhibitor.

(c) Conjugates of **I** with mPEG or ST-PHPMA inhibited cathepsin K activity in synovial fibroblasts. However, the ST-PHPMA−**I** conjugate was internalized faster with a concomitant increase in its biological activity when compared to the mPEG−**I** conjugate.

(d) One may hypothesize that these new lysosomotropic macromolecular inhibitors of cathepsin K may have potential in the treatment of osteoporosis and rheumatoid arthritis.

ACKNOWLEDGMENT

We thank Prof. Glenn Prestwich for the use of the microplate spectrofluorometer system. Helpful discussions on mass spectrometry data with Prof. James A. McCloskey and Dr. Vajira Nanayakara are also appreciated. Michal Pechar thanks the Institute of Macromolecular Chemistry, Academy of Sciences of the Czech Republic, for his leave of absence.

REFERENCES

1. Tezuka, K., Tezuka, Y., Maejima, A., Sato, T., Nemoto, K., Kamioka, H., Hakeda, Y., and Kumegawa, M. (1994) *J. Biol. Chem. 269*, 1106−1109.
2. Shi, G.-P., Chapman, H. A., Bhairi, S. M., DeLeeuw, C., Reddy, V. Y., Weiss, S. J. (1995) *FEBS Lett. 357*, 129−134.
3. Inaoka, T., Bilbe, G., Ishibashi, O., Tezuka, K., Kumegawa, M., and Kokubo, T. (1995) *Biochem. Biophys. Res. Commun. 206*, 89−96.
4. Li, Y. P., Alexander, M. B., Wucherpfennig, A. L., Chen, W., Yelick, P., and Stashenko, P. (1995) *J. Bone Miner. Res. 10*, 1197−1202.
5. Brömme, D., and Okamoto, K. (1995) *Biol. Chem. Hoppe-Seyler 376*, 379−384.
6. Brömme, D., Okamoto, K., Wang, B. B., and Biroc, S. (1996) *J. Biol. Chem. 271*, 2126−2132.
7. Drake, F. H., Dodds, R. A., James, I. E., Connor, J. R., Debouck, C., Richardson, S., Lee-Rykaczewski, E., Coleman, L., Rieman, D., Bartlow, R., Hastings, G., and Gowen, M. (1996) *J. Biol. Chem. 271*, 12511−12516.
8. Gelb, B. D., Shi, G.-P., Chapman, H. A., and Desnick, R. J. (1996) *Science 273*, 1236−1238.
9. Johnson, M. R., Polymeropoulos, M. H., Vos, H. L., Ortiz de Luna, R. I., and Francomano, C. A. (1996) *Genome Res. 6*, 1050−1055.
10. Inui, T., Ishibashi, O., Inaoka, T., Origane, Y., Kumegawa, M., Kokubo, T., and Yamamura, T. (1997) *J. Biol. Chem. 272*, 8109−8112.
11. Kafienah, W., Brömme, D., Buttle, D. J., Croucher, L. J., and Hollander, A. P. (1998) *Biochem. J. 331*, 727−732.
12. Garnero, P., Borel, O., Byrjalsen, I., Ferreras, M., Drake, F. H., McQueney, M. S., Foged, N. T., Delmas, P. D., and Delaisse, J.-M. (1998) *J. Biol. Chem. 273*, 32347−32352.
13. Hummel, K. M., Petrow, P. K., Franz, J. K., Muller-Ladner, U., Aicher, W. K., Gay, R. E., Brömme, D., and Gay, S. (1998) *J. Rheumatol. 25*, 1887−1894.
14. Hou, W., Li, Z., Gordon, R. E., Chan, K., Klein, M. J., Levy, R., Keysser, M., Keyszer, G., and Brömme, D. (2001) *Am. J. Pathol. 159*, 2167−2177.
15. Bobek, L. A., and Levine, M. J. (1992) *Crit. Rev. Oral Biol. Med. 3* (4), 307−332.
16. Guay, J., Falgueyret, J.-P., Ducret, A., Percival, M. D., and Mancini, J. A. (2000) *Eur. J. Biochem. 267*, 6311−6318.
17. Carmona, E., Dufour, E., Plouffe, C., Takebe, S., Mason, P., Mort, J. S., and Menard, R. (1996) *Biochemistry 35*, 8149−8157.
18. Yamashita, D. S., and Dodds, R. A. (2000) *Curr. Pharm. Des. 6*, 1−24.

19. Brömme, D., Klaus, J. L., Okamoto, K., Rasnick, D., and Palmer, J. T. (1996) *Biochem. J. 315*, 85−89.
20. Marquis, R. W., Ru, Y., LoCastro, S. M., Zeng, J., Yamashita, D. S., Oh, H.-J., Erhard, K. F., Davis, L. D., Tomaszek, T. A., Tew, D., Salyers, K., Proksch, J., Ward, K., Smith, B., Levy, M., Cummings, M. D., Haltiwanger, R. C., Trescher, G., Wang, B., Hemling, M. E., Quinn, C. J., Cheng, H. Y., Lin, F., Smith, W. W., Janson, C. A., Zhao, B., McQueney, M. S., D'Alessio, K., Lee, C.-P., Marzulli, A., Dodds, R. A., Blake, S., Hwang, S.-M., James, I. E., Gress, C. J., Bradley, B. R., Lark, M. W., Gowen, M., and Veber, D. F. (2001) *J. Med. Chem. 44*, 1380−1395.
21. LaLonde, J. M., Zhao, B., Smith, W. W., Janson, C. A., DesJarlais, R. L., Tomaszek, T. A., Carr, T. J., Thompson, S. K., Oh, H.-J., Yamashita, D. S., Veber, D. F., and Abdel-Meguid, S. S. (1998) *J. Med. Chem. 41*, 4567−4576.
22. DesJarlais, R. L., Yamashita, D. S., Oh, H.-J., Uzinskas, I. N., Erhard, K. F., Allen, A. C., Haltiwanger, R. C., Zhao, B., Smith, W. W., Abdel-Meguid, S. S., D'Alessio, K., Janson, C. A., McQueney, M. S., Tomaszek, T. A., Levy, M. A., and Veber, D. F. (1998) *J. Am. Chem. Soc. 120*, 9114−9115.
23. Yamashita, D. S., Dong, X., Oh, H.-J., Brook, C. S., Tomaszek, T. A., Szewczuk, L., Tew, D. G., and Veber, D. F. (1999) *J. Comb. Chem. 1*, 207−215.
24. Xia, L., Kilb, J., Wex, H., Li, Z., Lipyansky, A., Breuil, V., Stein, L., Palmer, J. T., Dempster, D. W., and Brömme, D. (1999) *Biol. Chem. 380*, 679−687.
25. Dodds, R. A., James, I. E., Rieman, D., Ahern, R., Hwang, S. M., Connor, J. R., Thompson, S. D., Veber, D. F., Drake, F. H., Holmes, S., Lark, M. W., and Gowen, M. (2001) *J. Bone Miner. Res. 16*, 478−486.
26. McQueney, M. S., Amegadzie, B. Y., D'Alessio, K., Hanning, C. R., McLaughlin, M. M., McNulty, D., Carr, S. A., Ijames, C., Kurdyla, J., and Jones, C. S. (1997) *J. Biol. Chem. 272*, 13955−13960.
27. Rieman, D. J., McClung, H. A., Dodds, R. A., Hwang, S. M., Holmes, M. W. L., James, I. E., Drake, F. H., and Gowen, M. (2001) *Bone 28*, 282−289.
28. Everts, V., Aronson, D. C., and Beertsen, W. (1985) *Calcif. Tissue Int. 37*, 25−31.
29. De Duve, C., De Barsy, T., Poole, B., Trouet, P., Tulkens, P., and van Hoof, F. (1974) *Biochem. Pharmacol. 23*, 2495−2531.
30. Kopeček, J., Kopečková, P., Minko, T., and Lu, Z. R. (2000) *Eur. J. Pharm. Biopharm. 50*, 61−81.
31. Maeda, H. (2001) *Adv. Drug Delivery Rev. 46(1−3)*, 69−185.
32. Duncan, R., Gac-Breton, S., Keane, R., Musila, R., Sat, Y. N., Satchi, R., and Searle, F. (2001) *J. Controlled Release 74(1−3)*, 35−146.
33. Palokangas, H., Mulari, M., and Väänänen, K. (1997) *J. Cell Sci. 110*, 1767−1780.
34. Pierce, W. M., Jr., and Waite, L. C. (1987) *Proc. Soc. Exp. Biol. Med. 186*, 96−102.
35. Fujisaki, J., Tokunaga, Y., Takahashi, T., Hirose, T., Shimojo, F., Kagayama, A., and Hata, T. (1995) *J. Drug Targeting 3*, 273−282.
36. Maeda, H. (2001) *Adv. Enzyme Regul. 41*, 189−207.
37. Fava, R. A., Olsen, N. J., Spencer-Green, G., Yeo, K.-T., Yeo, T.-K., Berse, B., Jackman, R. W., Senger, D. R., Dvorak, H. F., and Brown, L. F. (1994) *J. Exp. Med. 180* (1), 341−346.
38. Thompson, S. K., Halbert, S. M., Bossard, M. J., Tomaszek, T. A., Levy, M. A., Zhao, B., Smith, W. W., Abdel-Meguid, S. S., Janson, C. A., D'Alessio, K. J., McQueney, M. S., Amegadzie, B. Y., Hanning, C. R., DesJarlais, R. L., Briand, J., Sarkar, S. K., Huddleston, M. J., Ijames, C. F., Carr, S. A., Garnes, K. T., Shu, A., Heys, J. R., Bradbeer, J., Zembryki, D., Lee-Rykaczewski, L., James, I. E., Lark, M. W., Drake, F. H., Gowen, M., Gleason, J. G., and Veber, D. F. (1997) *Proc. Natl. Acad. Sci. U.S.A. 94*, 14249−14254.
39. Kopeček, J., and Bažilová, H. (1973) *Eur. Polym. J. 9*, 7−14.
40. Rejmanová, P., Labský, J., and Kopeček, J. (1977) *Makromol. Chem. 178*, 2159−2168.
41. Thompson, S. K., Smith, W. W., Zhao, B., Halbert, S. M., Tomaszek, T. A., Tew, D. G., Levy, M. A., Janson, C. A., D'Alessio, K. J., McQueney, M. S., Kurdyla, J., Jones, C. S., DesJarlais, R. L., Abdel-Meguid, S. S., and Veber, D. F. (1998) *J. Med. Chem. 41*, 3923−3927.
42. Lu, Z. R.; Kopečková, P.; Wu, Z.; and Kopeček, J. (1998) *J. Bioconjugate Chem. 9*, 793−804.
43. Knight, G. C. (1995) *Methods Enzymol. 248*, 85−101.
44. Williams, J. W., and Morrison, J. F. (1988) *Adv. Enzymol. 61*, 201−301.
45. Bossard, M. J., Tomaszek, T. A., Levy, M. A., Ijames, C. F., Huddleston, M. J., Briand, J., Thompson, S., Halpert, S., Veber, D. F., Carr, S. A., Meek, T. D., and Tew, D. G. (1999) *Biochemistry 38*, 15893−15902.
46. Tchoupé, J. R., Moreau, T., Gauthier, F., and Bieth, J. G. (1991) *Biochim. Biophys. Acta 1076*, 149−151.
47. Melo, R. L., Alves, L. C., Nery, E. D., Juliano, L., and Juliano, M. A. (2001) *Anal. Biochem. 293*, 71−77.
48. Szabelski, M., Stachowiak, K., and Wiczk, W. (2001) *Acta Biochim. Pol. 48* (4), 995−1002.
49. Musil, D., Zucic, D., Turk, D., Engh, R. A., Mayr, I., Huber, R., Popovic, T., Turk, V., Towatari, T., and Katunuma, N. (1991) *EMBO J. 10*, 2321−2330.
50. Kopeček, J., and Rejmanová, P. (1983) in *Controlled Drug Delivery Vol. I* (Bruck, S. D., Ed.) pp 81−124, CRC Press, Boca Raton, FL.
51. Kopeček, J., Rejmanová, P., and Chytrý, V. (1981) *Makromol. Chem. 182*, 799−809.
52. Kopeček, J., Cífková, I., Rejmanová, P., Strohalm, J., Obereigner, B., and Ulbrich, K. (1981) *Makromol. Chem. 182*, 2941−2949.
53. Duncan, R., Cable, H. C., Lloyd, J. B., Rejmanová, P., and Kopeček, J. (1983) *Makromol. Chem. 184*, 1997−2008.
54. Rejmanová, P., Kopeček, J., Pohl, J., Baudyš, M., and Kostka, V. (1983) *Makromol. Chem. 184*, 2009−2020.
55. Ulbrich, K., Strohalm, J., and Kopeček, J. (1986) *Makromol. Chem. 187*, 1131−1144.
56. Rejmanová, P., Obereigner, B., and Kopeček, J. (1981) *Makromol. Chem. 182*, 1899−1915.
57. Ulbrich, K., Strohalm, J., and Kopeček, J. (1981) *Makromol. Chem. 182*, 1917−1928.
58. Ulbrich, K., Zacharieva, E. I., Obereigner, B., and Kopeček, J. (1980) *Biomaterials 1*, 199−204.
59. Ulbrich, K., Strohalm, J., and Kopeček, J. (1982) *Biomaterials 3*, 150−154.
60. Harris, J. M. (1992) in *Poly(Ethylene Glycol) Chemistry, Biotechnical and Biomedical Applications* (Harris, J. M., Ed.) pp 1−12, Plenum Press, New York, N. Y.
61. Bohdanecký, M., Bažilová, H., and Kopeček, J. (1974) *Eur. Polym. J. 10*, 405−410.
62. Šubr, V., Duncan, R., Hanada, K., Cable, H. C., and Kopeček, J. (1986) *J. Controlled Release 4*, 63−68.

BI0257080